Theory of Segmental Orientation in Amorphous Polymer Networks

Burak Erman† and Lucien Monnerie*

Laboratoire de Physicochimie Structurale et Macromolêculaire, Associê au CNRS, ESPCI, 75231 Paris Cedex 05, France. *Received December 27, 1984*

ABSTRACT: A segmental orientation function for a deformed amorphous Gaussian network is formulated. The expression for the segmental orientation function is obtained as a product of two terms, the first relating to configurational properties of the chains and the second to the state of deformation of the network. The former term is obtained by using the statistical treatment of bond orientations in a chain of fixed end-to-end separation, initially formulated by Nagai. The second factor, showing the effect of macroscopic strain on segmental orientation, is formulated according to the recent theory of elasticitiy of real networks. Contributions of local intermolecular correlations to the segmental orientation function are also incorporated into the formulation. Application of the theory to interpretation of experimental spectroscopic techniques (such as infrared dichroism, deuterium NMR, and fluorescence polarization) is discussed. Numerical calculations are presented giving the dependence of the orientation function to network parameters and on the macroscopic state of strain. Orientation is found to be not proportional to the true stress, showing that stress cannot be employed as a measure of orientation.

Introduction

Recent developments in spectroscopic techniques allow accurate measurement of orientations of structural units in deformed polymeric systems.[1] Infrared dichroism (IRD), ^{2}H NMR spectroscopy, and fluorescence polarization (FP) are three methods that find increasing use in experimental investigations. These methods are based on the measurement of transformations of specific vectorial quantities with fixed positions relative to the chain segments such as dipole transition moment for IRD, C–D bonds for NMR and emission transition moment of fluorescent label for FP. Mean-squared projection of the specific vectors along a laboratory fixed axis in the deformed network is measured in experiments. The quantity of interest for theoretical investigations is the chain segment orientation, which may be related to the measured orientations of the specific vectors. If the specific vectors are either associated to each chain segment or to segments randomly distributed along the chains, their mean orientation will represent the mean orientation of the chain as a whole. In contrast, if the specific vectors are associated to segments that are localized in some defined part of the chain, their mean orientation will represent the mean orientation of these parts of the chains only.

Complete information on the orientation of investigated segments in a deformed network is obtained by knowledge of the orientational distribution function. Mean-squared projection of these segments along a given direction represents the second moment of the distribution. Data are generally presented in terms of the orientation function, S, defined as the second Legendre polynomial where

$$S = (3\langle\cos^2\theta\rangle - 1)/2 \quad (1)$$

where $\langle\cos^2\theta\rangle$ is the second moment showing mean-squared projection of the segment vectors on the laboratory fixed axis, θ being the angle between the segment vector and the axis.

Previous theories of orientation[2] lead to an expression for S that takes the following form for Gaussian networks

$$S = (1/5N)(\lambda^2 - \lambda^{-1}) \quad (2)$$

where N is the number of segments in a chain and λ is the deformation ratio. The expression for the orientation function given by (2) is conveniently separated into two factors. The prefactor $1/5N$ represents the statistical properties of chains and may be termed as the configurational factor. The second term, $\lambda^2 - \lambda^{-1}$, relates the orientation to macroscopic deformation and may be termed as the "strain function". Equation 2 is based on two assumptions. First, network chains are taken to be freely jointed. The indicated value of the configurational factor is obtained as a consequence of this assumption.[3] Second, network chains are assumed to deform affinely with macroscopic strain, leading to the strain function shown in (2). Non-Gaussian terms of order N^{-2} and higher, obtained by the theory,[2] are not included in (2) inasmuch as they are of vanishing importance for networks of sufficiently long chains.

Experimental and theoretical evidence shows that real chains are neither freely jointed[4] nor deform affinely in the network.[5,6] Consequently (2) stands as a crude approximation to the problem of segmental orientation. In this study, both the configuration and the strain terms are improved by adopting a real network model for orientation calculations. First, the hypothetical affine deformation condition is replaced by the more realistic concept of the nonaffine molecular state of deformation recently developed for the study of birefringence in a real network.[7] Secondly, the configuration term is corrected by replacing the freely jointed chain with its real analogue where averages are performed according to the rotational isomeric scheme. Calculation of the configuration term is extended to include effects of local steric intermolecular orientational correlations of segments with their environments. This latter effect has been experimentally observed in studies of orientation of networks by fluorescence polarization[8] and birefringence[9] and may contribute in an important way to segmental orientation.

In the first section below, the molecular structure of real networks is reviewed, and parameters affecting the orientation of segments under strain are discussed. In the second section, the state of average microscopic strain at the molecular level is related to the macroscopic state of strain by using molecular theory. The relationship of segmental orientation to the microscopic and macroscopic state of strain is described in the third section, followed by a discussion of contributions to orientation by specific local intermolecular correlations. Segmental orientation in uniaxially deformed networks, a special case of interest in experimental analysis, is formulated and numerical

† Permanent address: Bogazici University, Bebek, Istanbul, Turkey.

0024-9297/85/2218-1985$01.50/0

calculations are presented in the final section.

Molecular Theory of Real Networks

We assume that the network contains ν chains connected to each other at μ junctions of functionality φ, forming ξ cyclic circuits that contribute to stress under deformation. Two relations exist[10] between ν, μ, φ, and ξ:

$$\xi = \mu(\varphi - 2)/2 \qquad \nu = \mu\varphi/2 = \xi/(1 - 2/\varphi) \tag{3}$$

thus leaving only two free molecular parameters for the characterization of the network structure. Equation 3 may be used to explain imperfect as well as perfect networks. For the former, μ and ν denote the effective numbers of junctions and chains, respectively.

Gaussian statistics of the network[10,11] lead to interrelations between the mean-squared values of the chain end-to-end length, $\langle r^2 \rangle$, fluctuations in the chain dimensions, $\langle (\Delta r)^2 \rangle$, and fluctuations in the positions of junctions from their mean locations, $\langle (\Delta R)^2 \rangle$, where brackets denote the ensemble average. In the state of rest, denoted by the subscript 0, the following relations hold for a phantom network:

$$\langle (\Delta r)^2 \rangle_0 = 2\langle r^2 \rangle_0/\varphi \tag{4a}$$

$$\langle (\Delta R)^2 \rangle_0 = [(\varphi - 1)/\varphi(\varphi - 2)]\langle r^2 \rangle_0 \tag{4b}$$

Ordinarily, the junction functionality and the number of junctions in a network are specified at the outset. An "average" tetrafunctional network contains on the order of 3×10^{19} junctions/mL, which corresponds to a molecular weight of ca. 10^4 for a chain between two cross-links. A chain of this length contains about 400 bonds. If the bond length is 1.5 Å and the characteristic ratio for the chain is 6, the radius, $\langle r^2 \rangle_0^{1/2}$, of the volume occupied by the chain will be 70 Å. There will be approximately 40 junctions in the domain occupied by each chain. From (4a), the mean radius of the fluctuation domain, $\langle (\Delta r)^2 \rangle_0^{1/2}$, will be 50 Å, and from (4b), the average fluctuation distance, $\langle (\Delta R)^2 \rangle_0^{1/2}$, of a junction from its mean position will be about 40 Å.

The degree of interpenetration depends on the number of junctions in the domain of a chain. Entanglement of chains in the deformed network will perturb the distribution of the chain dimensions. The constraints due to entanglements are introduced into the theory by means of "springlike" forces acting on the fluctuating junctions. For each junction, a center of constraint is defined. The deviation of the real network from the corresponding phantom analogue is represented in the theory by the parameter κ defined as

$$\kappa = \langle (\Delta R)^2 \rangle_{ph}/\langle (\Delta s)^2 \rangle_0 \tag{5}$$

where $\langle (\Delta R)^2 \rangle_{ph}$ refers to the phantom network and $\langle (\Delta s)^2 \rangle_0$ is the mean-squared fluctuation of junctions from their constraint centers. For the tetrafunctional network example given above, typical values of κ obtained from experimental data lie in the range of 6–10. From (5) with $\kappa = 8$, we obtain $\langle (\Delta s)^2 \rangle_0^{1/2} = 15$ Å. Inasmuch as the mean radius of the volume per junction in the network is of the same order as $\langle (\Delta s)^2 \rangle_0^{1/2}$, the fluctuations of junctions from their constraint centers will be confined, on the average, to the domain allocated to each junction. Similar calculations on networks of different cross-link densities lead to the same conclusion. The constraints affecting junctions in the manner stated above also affect portions of the chains situated within the domain of each junction. This follows directly from the postulate of the theory of real networks that junctions and their environments are elastically coupled.

The structure of real networks described in the above paragraphs directly affects the configurations of chains in the deformed network. The deformation field to which chains are subjected is not affine in the macroscopic strain but depends on the degree of constraints acting on junctions as shown quantitatively in the next section. Furthermore, segments are subjected to a local deformation field caused by the distortion of the constraint domains.

Relationship between Macroscopic and Microscopic States of Deformation

Let a network be subjected to a homogeneous state of macroscopic deformation, expressed by the displacement gradient tensor, λ, and the macroscopic deformation tensor, $\lambda^T\lambda$. Here, the superscript T denotes the transpose. In the sequel we assume, for simplicity, that the tensor λ is expressed in the laboratory fixed principal coordinate system $0xyz$, in which only the diagonal elements of λ are nonzero. The state of deformation at the molecular scale may be defined by a deformation gradient tensor, Λ^2, given as

$$\Lambda^2 = \begin{bmatrix} \langle x^2 \rangle/\langle x^2 \rangle_0 & 0 & 0 \\ 0 & \langle y^2 \rangle/\langle y^2 \rangle_0 & 0 \\ 0 & 0 & \langle z^2 \rangle/\langle z^2 \rangle_0 \end{bmatrix} \tag{6}$$

where $\langle x^2 \rangle$, $\langle y^2 \rangle$, and $\langle z^2 \rangle$ are the three Cartesian components of the mean-squared end-to-end vector, $\langle r^2 \rangle$, in the deformed state. The averages with the subscript zero refer to the corresponding components of $\langle r^2 \rangle$ in the state of rest.

Statistical treatment of chain end-to-end vectors in the real network leads to the expression relating the components of Λ^2 to λ,

$$\Lambda_t^2 = (1 - 2/\varphi)\lambda_t^2 + (2/\varphi)(1 + B_t) \tag{7}$$

Here

$$B_t = (\lambda_t - 1)(\lambda_t + 1 - \zeta\lambda_t^2)/(1 + g_t)^2 \tag{8}$$

with

$$g_t = \lambda_t^2[\kappa^{-1} + \zeta(\lambda_t - 1)] \tag{9}$$

where t denotes x, y, or z.

In (8) and (9), κ is the previously defined interpenetration parameter; ζ is a parameter introduced[5] in order to account for the experimental data on dry and swollen networks. It describes a stronger disappearance of constraints with strain or swelling.

Equation 7 relates the *mean* deformation (according to the ensemble distribution) of chains of the network to the macroscopic deformation. For a phantom network, $\kappa = 0$, $B_t = 0$, and

$$\Lambda_t^2 = (1 - 2/\varphi)\lambda_t^2 + 2/\varphi \tag{10}$$

The phantom network represents one extreme for which the effect of constraints is null. In the opposite extreme, where constraints suppress the fluctuations of chains completely, corresponding to the case of affine deformation, $\kappa = \infty$ and $\zeta = 0$, leading to

$$\Lambda_t^2 = \lambda_t^2 \tag{11}$$

Equations 10 and 11 represent lower and upper bounds, respectively, for the components of the molecular deformation tensor.

Furthermore, the fluctuation domains of junctions transform in the presence of chain connectivity. This creates an additional strain field in the medium around

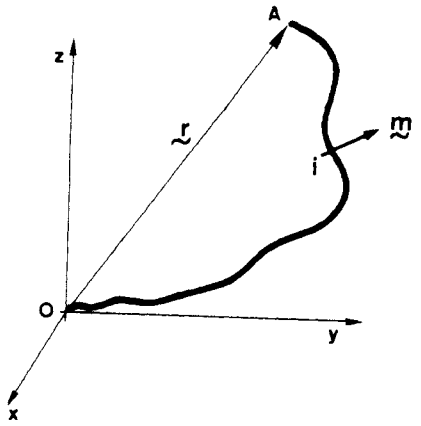

Figure 1. Given configuration of a chain with the vector **m** attached at point i. **r** denotes the end-to-end vector. The coordinate system 0*xyz* shown is the laboratory fixed system referred to in the text.

each junction. Contributions from this source may be explained in terms of the instantaneous fluctuation vector, $\Delta\mathbf{S}$, of a junction from its center of constraint. $\Delta\mathbf{S}$ is assumed to transform with macroscopic deformation. We let $\Delta\mathbf{S}_*$ represent the fluctuation of the junction from its constraint center, under the combined effects of constraints and network connectivity, in the deformed network. The subscript * acknowledges the effect of connectivity. The difference between the distribution of $\Delta\mathbf{S}$ and $\Delta\mathbf{S}_*$ obtained by the statistical treatment of junction fluctuations[5] leads to a state of deformation not accounted for by Λ^2. Accordingly, we define a junction domain deformation tensor Θ^2 by

$$\Theta^2 = \begin{bmatrix} \langle(\Delta S_x)_*^2\rangle/\langle(\Delta S_x)^2\rangle & 0 & 0 \\ 0 & \langle(\Delta S_y)_*^2\rangle/\langle(\Delta S_y)^2\rangle & 0 \\ & & \langle(\Delta S_z)_*^2\rangle/\langle(\Delta S_z)^2\rangle \end{bmatrix} \tag{12}$$

Components of Θ^2 are related to the macroscopic deformation tensor λ according to the theory by

$$\Theta_t^2 = 1 + g_t B_t \tag{13}$$

Θ^2 relates the *mean* deformation (according to ensemble distribution) of the junction constraint domains in the deformed, connected network to that in the absence of connectivity.

Consequently, the state of microscopic deformation in a real network is the combination of the molecular deformation tensor, Λ^2, whose components are given by (7) and the junction domain deformation tensor, Θ^2, whose components are given by (13). In the two extreme cases of phantom and affine networks, the contribution from the junction domain deformation disappears.

Relation of Segmental Orientation to Deformation in a Network

A chain of the network between two cross-links is shown schematically in Figure 1 with respect to the laboratory fixed-coordinate system 0*xyz*. The heavy line represents the instantaneous contour of the chain. $\mathbf{r} = \mathbf{OA}$ represents the corresponding end-to-end vector. A vector **m** is affixed to the chain at a specific location i as shown in the figure. The direction of **m** may not coincide with that of the bond to which it is attached.

We assume that the angle between **m** and the x axis is Θ for the configuration shown, and the angle between **m** and **r** is Φ.

For the specified position of **r**, the segments of the chain will assume different conformations. The angles θ and Φ will accordingly take different values. The value of $\cos^2\theta$ averaged over all conformations of the chain subject to the constancy of **r** is derived by Nagai[12] as

$$\overline{\cos^2\theta} = [1 + 3D_0(3x^2/\langle r^2\rangle_0 - r^2/\langle r^2\rangle_0)]/3 \tag{14}$$

where

$$D_0 = (3\langle r^2\cos^2\Phi\rangle_0/\langle r^2\rangle_0 - 1)/10 \tag{15}$$

The subscript zero in (14) and (15) denotes the free state of the chains. It has been shown by Nagai that D_0 defined by (15) is of the order of $1/n$, where n is the number of segments of the chain. Terms of order $1/n^2$ and higher that are included in Nagai's treatment are omitted from the right-hand side of (14). Inasmuch as n will be larger than 100 in the type of networks under discussion, contributions of terms of $O(1/n^2)$ to $\cos^2\theta$ will be negligibly small. The expression $\langle r^2\cos^2\Phi\rangle_0$ may be calculated according to matrix generation techniques and the rotational isomeric state formalism[3] as shown in the Appendix.

The orientation function for the vector **m** in the chain is obtained from (14) and the definition given by (1) as

$$\bar{S}_x = (3D_0/2)(3x^2/\langle r^2\rangle_0 - r^2/\langle r^2\rangle_0) \tag{16}$$

The overbar denotes that the orientation function refers to a single chain and not to an ensemble of chains. The subscript x is appended to S in (16) to show that the orientation function is with respect to the x-axis.

In order to obtain the mean orientation function for an ensemble of vectors **m** in a network, the manner in which the vectors are attached to the chains should be specified clearly. We first assume that a vector **m** is affixed to the same specific location along each chain. The value of D_0 in (16) is then the same for every chain. Taking the ensemble average of both sides of (16), we obtain

$$S_x' = D_0[\langle x^2\rangle/\langle x^2\rangle_0 - (\langle y^2\rangle/\langle y^2\rangle_0 + \langle z^2\rangle/\langle z^2\rangle_0)/2] \tag{17}$$

where the relations $\langle x^2\rangle_0 = \langle y^2\rangle_0 = \langle z^2\rangle_0 = \langle r^2\rangle_0/3$ have been used for the isotropic undisturbed state of the network and the prime indicates that the anisotropy of the distribution is due to transformations of the network chains under macroscopic strain described by the molecular deformation tensor, Λ^2 (see the following paper in this series[18] for the additional effect of junction constraint domains denoted by double prime). Substituting from (6) into (17) we obtain

$$S_x' = D_0[\Lambda_x^2 - (\Lambda_y^2 + \Lambda_z^2)/2] \tag{18}$$

The second contribution to the orientation function arises from the distortion of the junction constraint domains. Indeed, depending on the extent of distortion, chains surrounding a given junction have to reorganize at a scale corresponding to the size of its constraint domain. This results in an additional orientation of the segments present in the domain. Accordingly, we expect a further orientation of vector **m** proportional to the local domain deformation tensor. In analogy with (18), we write, therefore,

$$S_x'' = eD_0[\Theta_x^2 - (\Theta^2_y + \Theta^2_z)/2] \tag{19}$$

where e denotes the strength of reaction of **m** to the distortion of the junction constraint domain.

The total contribution to the orientation function will be obtained as the sum of (18) and (19) as[13]

$$S_x = D_0\{\Lambda_x^2 - (\Lambda_y^2 + \Lambda_z^2)/2 + e[\Theta_x^2 - (\Theta_y^2 + \Theta_z^2)/2]\} \tag{20}$$

In (20), D_0 denotes the configurational factor. In the case where each experimentally observed chain contains a single vector **m** attached to a specific segment, D_0 is related to configurational averages by (15). Its calculation for a given system is outlined in the Appendix.

If several vectors are affixed to a chain, each designated by $\mathbf{m}_i$, i denoting the specific location along the chain, the expression for S remains the same as that given by (20) where D_0 has to be redefined as

$$D_0 = \sum_{i=1}^{k} D_{0i}/k \tag{21}$$

with

$$D_{0i} = (3\langle r^2 \cos^2 \Phi_i\rangle_0/\langle r^2\rangle_0 - 1)/10 \tag{15'}$$

Here, k denotes the total number of sites on the chain to which the vectors are attached, and Φ_i denotes the angle between $\mathbf{m}_i$ and **r**.

If a single vector **m** is affixed to a random location i on a chain, the expression for S remains the same as that given by (20) with D_0 defined as in (21) and k denoting the number of possible sites on the chain.

Effect of Local Intermolecular Correlations

Experimental work on birefringence of amorphous networks has shown that the stress optical coefficient of dry networks leads to values of optical anisotropies that are much higher than those calculated for the single chain according to the rotational isomeric state approximation.[9,14] The enhancement of polarizabilities in the bulk originates from local intermolecular orientational correlations of first-neighbor segments in the densely packed medium. The fact that these correlations affect local orientation of segments but not the overall chain configurations has been demonstrated by several independent experiments.[15] Such intermolecular correlations are also observed in fluorescence polarization experiments[8] and in depolarized Rayleigh scattering measurements on higher n-alkanes and has been attributed to two mechanisms:[17] (i) intermolecular steric constraints (due to uncrossability of chains) hinder rotations of neighboring segments about each other and (ii) neighboring chains tend to align with respect to each other due to anisotropic intermolecular dispersive forces. All experiments measuring local orientational correlation have shown that the effect sharply diminishes with dilution by an isotropic solvent or with increasing temperature.

The effect of intermolecular correlations on segment orientation of a chain in the bulk will affect the term $\langle r^2 \cos^2 \Phi\rangle$ in the expression for D_0, given by (15) for an isolated free chain. In this latter case, the angle Φ is unbiased by intermolecular perturbations according to the basic postulate of statistical mechanics of free chains.[4] In the presence of intermolecular correlations, the angle Φ at each conformation of the chain is expected to differ from the one obtained in the free chain. The expression for the configurational factor may be written in the presence of correlations as

$$D = [3\langle(\mathbf{ru})^2\rangle/\langle r^2\rangle - 1]/10 \tag{22}$$

where **u** is a unit vector along **m** in the perturbed conformation. Denoting the unit vector along **m** in the absence of correlations by $\mathbf{u}_0$ and the difference between $\mathbf{u}_0$ and **u** by $\Delta\mathbf{u}$, we have

$$D = [(3\langle r^2 \cos^2 \Phi\rangle/\langle r^2\rangle - 1)/10 + 3\langle \Delta\mathbf{u}^2 \cos^2 \delta\rangle/10] \tag{23}$$

where δ denotes the angle between $\Delta\mathbf{u}$ and **r**. Equation 23 is derived on the assumption that perturbations $\Delta\mathbf{u}$ are not correlated with **r**, which should be the case for weak local correlations considered in the present study.

The first term in the square brackets in (23) refers to the configurational factor, D_0, given by (15) for the free chain. Hence we may write

$$D = D_0 + D_{\text{int}} \tag{24}$$

where $D_{\text{int}} = 3\langle \Delta\mathbf{u}^2 \cos^2 \delta\rangle/10$ is the intermolecular contribution to the total orientation factor, D.

The effect of local intermolecular correlations on segmental orientation in a deformed amorphous network has previously been derived by Jarry and Monnerie,[2h] using a different approach. The present formulation and theirs may be brought into correspondence if

$$\frac{D_{\text{int}}}{D_0} = \frac{V}{1 - V} \tag{25}$$

where V defines the intensity of interaction between orientations of neighboring segments according to their formulation.

Incorporation of local correlations into the orientation function affects only the configurational factor. The strain function is unaffected by such correlations. Thus, the most general expression for the orientation function, S, takes the form

$$S_x = (D_0 + D_{\text{int}}) \times \{\Lambda_x^2 - (\Lambda_y^2 + \Lambda_z^2)/2 + e[\Theta_x^2 - (\Theta_y^2 + \Theta_z^2)/2]\} \tag{20a}$$

Segmental Orientation in a Uniaxially Deformed Network

The state of deformation of a network obtained under a uniaxial force along the x-direction is expressed by

$$\lambda = \begin{bmatrix} \lambda & 0 & 0 \\ 0 & (v_2/\lambda)^{1/2} & 0 \\ 0 & 0 & (v_2/\lambda)^{1/2} \end{bmatrix} \tag{26}$$

$$= \begin{bmatrix} v_2^{-1/3}\alpha & 0 & 0 \\ 0 & v_2^{-1/3}\alpha^{-1/2} & 0 \\ 0 & 0 & v_2^{-1/3}\alpha^{-1/2} \end{bmatrix} \tag{26a}$$

The matrices in (26) and (26a) include the effect of swelling on deformation, where v_2 indicates the volume fraction of polymer in the swollen system, λ is the ratio of the swollen deformed length to the unswollen, undeformed length, and α is the ratio of the swollen deformed length to swollen undeformed length. Substituting (26a) into (7) and (12) and the resulting expression into (20a), we obtain the orientation function as

$$S_x = (1 - 2/\varphi)v_2^{-2/3}D[(\alpha^2 - \alpha^{-1}) + 2v_2^{2/3}(\varphi - 2)^{-1}\{B_1 - B_2 + (\varphi e/2)(g_1B_1 - g_2B_2)\}] \tag{27}$$

where D is defined by (24).

For a phantom network, the second term in square brackets vanishes, and we obtain

$$S_{x,\text{ph}} = (1 - 2/\varphi)v_2^{-2/3}D(\alpha^2 - \alpha^{-1}) \tag{28}$$

The difference between (27) and (28) reflects the effect of the junction constraints on segmental orientation in networks.

The expression for S_x given by (27) resembles the one for strain birefringence obtained previously,[7] with the major difference that the total birefringence of a network is proportional to the number of network chains whereas the orientation function is independent of this extensive variable.

The expression for the orientation function given by (27) is fundamentally different from all previous formulations.[2]

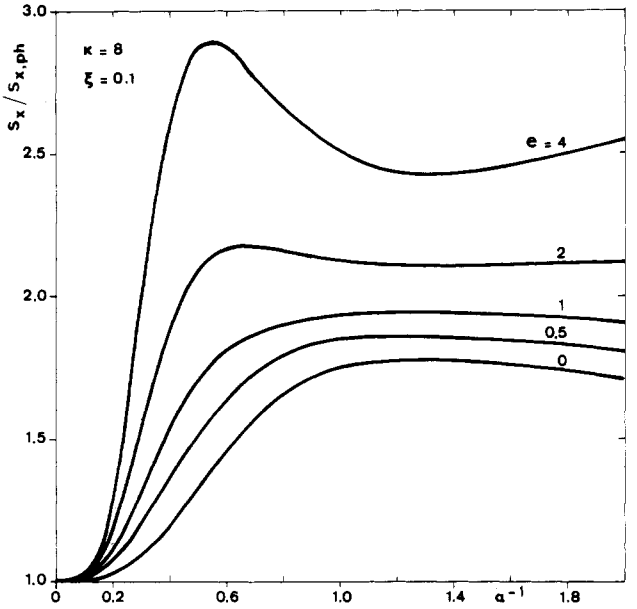

Figure 2. Values of the ratio of the orientation function S_x of the real network to that of the phantom network, $S_{x,ph}$, plotted as a function of reciprocal extension ratio, α^{-1}. Results of calculations for $\kappa = 8$ and $\xi = 0.1$ are shown for various values of e, which measures the degree of elastic coupling between the segments and the constraint domain.

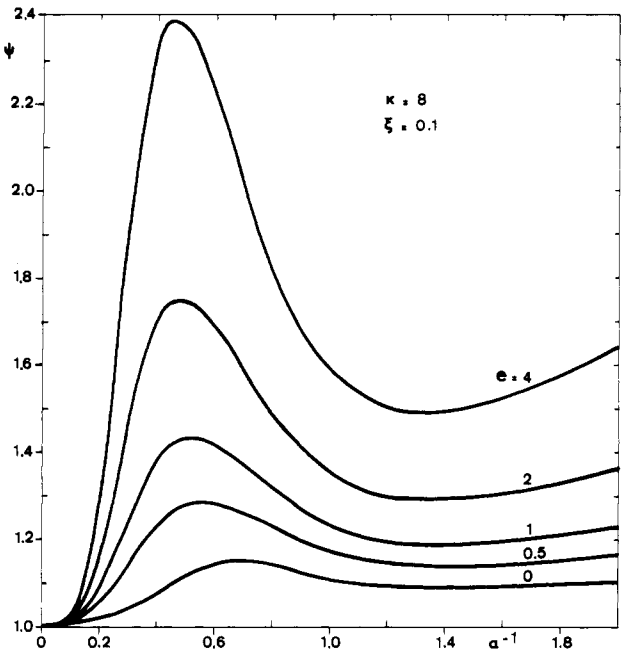

Figure 3. Values of $\psi = (S_x/S_{x,ph})/[(\tau_x - \tau_y)/(\tau_x - \tau_y)_{ph}]$ plotted as a function of α^{-1}. τ_x and τ_y denote the true stress parallel and perpendicular to stretching direction respectively. (See legend to Figure 2).

The configurational factor is introduced for a real chain whereas previous formulations treat the freely jointed chain only. The strain function of (27) is obtained for a Gaussian network whose chains transform nonaffinely under the influence of elastic constraints. Deviations from $(\lambda^2 - \lambda^{-1})$ dependence of orientation in all other theories result from the non-Gaussian nature of the chains. It should be noted that non-Gaussian terms are of order $1/N^2$ and higher and are negligible for networks with sufficiently long chains.

Numerical Calculations

In Figure 2, the ratio of the orientation function in a real tetrafunctional network to that in the phantom network is plotted for $\kappa = 8$, $\zeta = 0.1$, and different values of e. The curves are obtained by calculating the ratio of (27) to (28). The curve with $e = 0$ shows the effect of changes in chain dimensions on segmental orientation in a real network in the absence of the effect of junction domain deformation.

Strong contributions from the latter effect are obtained by increasing e, as is evident from the figure. The maxima in the curves shift to higher values of α as e increases. When $\alpha = 2$, the orientation function for $e = 4$ is about three times that for the phantom network. Results of calculations also show that the ratio $S_x/S_{x,ph}$ is approximately insensitive to strain for uniaxial compression. For high tensile strains, the orientation function of the real networks converges to that of the phantom network.

The ratio of the orientation function to the stress acting on the network gives an estimate of the relationship of orientation to stress. In order to obtain the ratio from the theory, we introduce the difference between the principal components of the true stress along the longitudinal (x) and the lateral (y) directions of deformation as[7]

$$\tau_x - \tau_y = (\xi kT/V)\{\lambda_x^2 - \lambda_y^2 + [\lambda_x^2 K(\lambda_x^2) - \lambda_y^2 K(\lambda_y^2)]/(\varphi/2 - 1)\} \quad (29)$$

where

$$K(\lambda^2) = B[\dot{B}(B + 1)^{-1} + g(\dot{g}B + g\dot{B})(gB + 1)^{-1}] \quad (30)$$

with

$$\dot{B} \equiv \partial B/\partial\lambda^2 = B\{[2\lambda(\lambda - 1)]^{-1} + (1 - 2\xi\lambda) \times [2\lambda(1 + \lambda - \xi\lambda^2)]^{-1} - 2\dot{g}(1 + g)^{-1}\} \quad (31)$$

and

$$\dot{g} \equiv \partial g/\partial\lambda^2 = \kappa^{-1} + \zeta(1 - 3\lambda/2) \quad (32)$$

λ_x and λ_y in (29) represent the longitudinal and lateral components, respectively, of the deformation gradient tensor. For the phantom network, (29) simplifies to

$$(\tau_x - \tau_y)_{ph} = (\xi kT/V)(\lambda_x^2 - \lambda_y^2) \quad (33)$$

The ratio, ψ, of the orientation function to the stress difference, both normalized with respect to the respective phantom contribution, is defined as

$$\psi = [S_x/S_{x,ph}]/[(\tau_x - \tau_y)/(\tau_x - \tau_y)_{ph}] \quad (34)$$

Substituting from (27), (28), (29), and (33) into (34) leads to the value of ψ. Results of calculations performed on this basis are shown in Figure 3 for $\kappa = 8$, $\zeta = 0.1$, and several values of e. Results indicate that ψ exhibits pronounced maxima between $\alpha = 1.5$ and 2.5, and its magnitude depends strongly on e. Values of ψ are less sensitive to uniaxial compressive strains. A local minimum is observed in the vicinity of $\alpha = 0.75$ for $e = 2$ and 4. A very shallow minimum also exists around the same value of α for lower values of e.

The above calculations indicate that orientation is not proportional to stress in real networks, thereby showing that stress cannot be adopted as a measure of orientation. The same conclusion has recently been reached both theoretically and experimentally for the relationship of birefringence to stress.[7,9]

The effect of swelling on orientation is shown in Figure 4 where values of $S_x/S_{x,ph}$ are calculated as a function of v_2. Values of κ and ξ are taken as 8 and 0.1, respectively. Results of calculations for different networks with values of e are shown. Calculations are made for $\alpha = 1.01$, which

$$\mathbf{Q}_i = \begin{bmatrix} \mathbf{U} & (\mathbf{U} \oplus \mathbf{l}^T)\|\mathbf{T}\| & (\mathbf{U} \oplus \mathbf{M}^R)\|\mathbf{T} \oplus \mathbf{T}\| & \frac{1}{2}(\mathbf{U} \oplus \mathbf{l}^T \oplus \mathbf{l}^T)\|\mathbf{T} \oplus \mathbf{T}\| & \mathbf{U} \oplus [\mathbf{M}^R(\mathbf{l} \oplus \mathbf{E}_3)]\|\mathbf{T}\| & \frac{1}{2}\mathbf{U}[\mathbf{M}^R(\mathbf{l} \oplus \mathbf{l})] \\ \mathbf{0} & (\mathbf{U} \oplus \mathbf{E}_3)\|\mathbf{T}\| & \mathbf{0} & (\mathbf{U} \oplus \mathbf{E}_3 \oplus \mathbf{l}^T)\|\mathbf{T} \oplus \mathbf{T}\| & (\mathbf{U} \oplus \mathbf{M})\|\mathbf{T}\| & \mathbf{U} \oplus [(\mathbf{E}_3 \oplus \mathbf{l}^T)\mathbf{M}^C] \\ \mathbf{0} & \mathbf{0} & (\mathbf{U} \oplus \mathbf{E}_9)\|\mathbf{T} \oplus \mathbf{T}\| & \mathbf{0} & (\mathbf{U} \oplus \mathbf{l} \oplus \mathbf{E}_3)\|\mathbf{T}\| & \frac{1}{2}(\mathbf{U} \oplus \mathbf{l} \oplus \mathbf{l}) \\ \mathbf{0} & \mathbf{0} & \mathbf{0} & (\mathbf{U} \oplus \mathbf{E}_9)\|\mathbf{T} \oplus \mathbf{T}\| & \mathbf{0} & \mathbf{U} \oplus \mathbf{M}^C \\ \mathbf{0} & \mathbf{0} & \mathbf{0} & \mathbf{0} & (\mathbf{U} \oplus \mathbf{E}_3)\|\mathbf{T}\| & \mathbf{U} \oplus \mathbf{l} \\ \mathbf{0} & \mathbf{0} & \mathbf{0} & \mathbf{0} & \mathbf{0} & \mathbf{U} \end{bmatrix} \quad \text{(A8)}$$

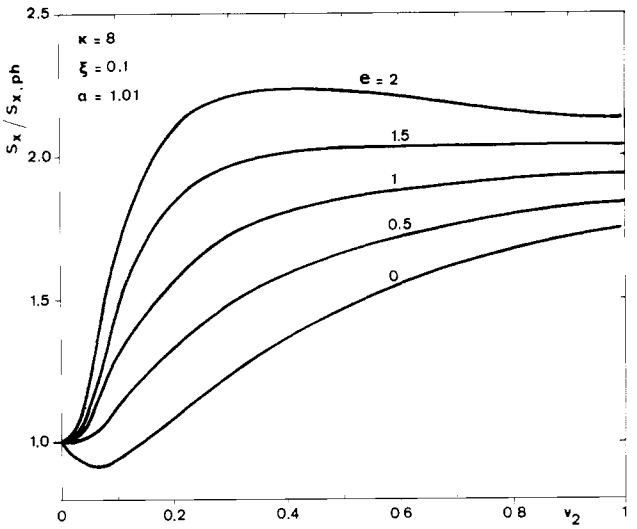

Figure 4. Variation of the ratio $S_x/S_{x,ph}$ with swelling, calculated for $\alpha = 1.01$. (See legend to Figure 2).

corresponds to the case of a very small uniaxial extension. Deviations of the orientation function in the real networks are high for small degrees of dilution ($v_2 \rightarrow 1$). The phantom behavior is approached as dilution increases. The curves with $e = 0$ and 0.5 show minima at high degrees of dilution. The curve with $e = 1.5$ remains approximately constant over a very large range of v_2 ($0.4 < v_2 < 1$) and then sharply converges to unity. The value of S_x is about twice that of the phantom $S_{x,ph}$ function, as can be seen from the figure. For $e = 2$, the ratio $S_x/S_{x,ph}$ shows a slight increase in the region $0.4 < v_2 < 1$. It converges sharply to unity for smaller values of v_2. The behavior of $S_x/S_{x,ph}$ for different values of α calculated but not shown is similar to that depicted in Figure 4.

Predictions of the present theory will be compared with results of fluorescence polarization experiments on polyisoprene networks in uniaxial tension.[18]

Acknowledgment. We acknowledge Professor P. J. Flory for helpful discussions.

Appendix A: Evaluation of D_0

The expression for D_0 given by (15) contains the average $\langle r^2 \cos^2 \Phi \rangle_0$, the calculation of which is outlined below according to the rotational isomeric state formalism. In order to benefit from the formulation previously obtained for birefringence,[4] we assume that a vector $\mathbf{m}_i$ of unit length is affixed to each repeat unit i of the chain whose end-to-end separation is fixed at $\mathbf{r}$. Then

$$r^2 \cos^2 \Phi_i = (\mathbf{r} \cdot \mathbf{m}_i)^2 \quad \text{(A1)}$$

where r is the magnitude of $\mathbf{r}$, and Φ_i is the angle between $\mathbf{m}_i$ and $\mathbf{r}$. Equation A1 can be expressed as

$$(\mathbf{r} \cdot \mathbf{m}_i)^2 = \mathbf{r}^T \mathbf{M}_i \mathbf{r} \quad \text{(A2)}$$

where $\mathbf{M}_i$ is the 3×3 matrix given by

$$\mathbf{M}_i = \mathbf{m}_i^T \otimes \mathbf{m}_i \quad \text{(A3)}$$

Here $\otimes$ denotes the direct product.

The average orientation of the vectors $\mathbf{m}_i$ may be obtained by the rotational isomeric state scheme, according to which

$$\sum_i \langle r^2 \cos^2 \Phi_i \rangle = \sum_i \langle \mathbf{r}^T \mathbf{M}_i \mathbf{r} \rangle = 2Z^{-1} \mathbf{J}^* \prod_{i=1}^{n} \mathbf{Q}_i \mathbf{J} \quad \text{(A4)}$$

where Z is the configuration partition function defined as the product of the statistical weight matrices, $\mathbf{U}$. Accordingly

$$Z = \prod_{i=1}^{n} \mathbf{U}_i \quad \text{(A5)}$$

with

$$\mathbf{U}_1 = \text{row } (1,0,0)$$
$$\mathbf{U}_n = \text{column } (1,1,1) \quad \text{(A6)}$$

In (A4), the remaining terms are

$$\mathbf{J}^* = \text{row } (1,0,0, \ldots)$$
$$\mathbf{J} = \text{column } (1,1,1, \ldots) \quad \text{(A7)}$$

and $\mathbf{Q}_i$ as defined by (A8). In (A8)

$$\|\mathbf{T}_i\| = \begin{bmatrix} T(\varphi_1) & & \\ & T(\varphi_2) & \\ & & T(\varphi_3) \end{bmatrix} \quad \text{(A9)}$$

and $\mathbf{M}^C$ = column form of M; $\mathbf{M}^R$ = row form of M; $\mathbf{E}_q$ = q' order identity matrix; and $\mathbf{E}_3$ = 3′ order identity matrix.

If there is only one vector $\mathbf{m}_i$ at the ith segment, (A4) simplifies to

$$\langle r^2 \cos^2 \Phi_i \rangle_i = 2Z^{-1} \mathbf{J}^* (\prod_{k=1}^{i-1} \mathbf{Q}_k') \mathbf{Q}_i \prod_{k=i+1}^{n} \mathbf{Q}_k' \quad \text{(A10)}$$

where $\mathbf{M}_k = 0$ in $\mathbf{Q}_k'$.

References and Notes

(1) See, for example: (a) Ward, I. M. "Structure and properties of oriented polymers"; Applied Science: London, 1975. (b) Monnerie, L. *Faraday Symp. Chem. Soc.* **1983**, *18*, 57.

(2) (2) See, for example: (a) Kuhn, W.; Grün, F. *Kolloid-Z.* **1942**, *101*, 248. (b) Treloar, L. R. G. *Trans. Faraday Soc.* **1947**, *43*, 277. (c) Isihara, A.; Hashitsume, N.; Tatibana, M. *J. Appl. Phys.* **1952**, *23*, 308. (d) Hermans, J. J. *J. Colloid Sci.* **1946**, *1*, 235. (e) Treloar, L. R. G. *Trans. Faraday Soc.* **1954**, *50*, 881. (f) Roe, R. J.; Krigbaum, W. R. *J. Appl. Phys.* **1964**, *35*, 2215. (g) Tanaka, T.; Allen, G. *Macromolecules* **1977**, *10*, 426. (h) Jarry, J. P.; Monnerie, L. *Macromolecules* **1979**, *12*, 316.

(3) The value of the configurational factor is obtained as $1/5N$ for the freely jointed chain with no specific local intermolecular correlations among chains. In the presence of interactions, according to ref 2g and 2h, the configurational factor becomes $1/5N(1 - V)$ where V is the strength of interactions.

(4) Flory, P. J. "Statistical Mechanics of Chain Molecules"; Interscience: New York, 1969.

(5) Flory, P. J.; Erman, B. *Macromolecules* **1982**, *15*, 800.

(6) Erman, B.; Flory, P. J. *Macromolecules* **1982**, *15*, 806.

(7) Erman, B.; Flory, P. J. *Macromolecules* **1983**, *16*, 1601.

(8) Jarry, J. P.; Monnerie, L. *J. Polym. Sci., Polym. Phys. Ed.* **1980**, *18*, 1879.

(9) Erman, B.; Flory, P. J. *Macromolecules* **1983**, *16*, 1607.
(10) Flory, P. J. *Proc. R. Soc. London, A.* **1976**, *351*, 351.
(11) Flory, P. J. *J. Chem. Phys.* **1977**, *66*, 5720.
(12) Nagai, K. *J. Chem. Phys.* **1964**, *40*, 2818.
(13) The orientation function is a second order tensor. It can be expressed in tensor form in terms of principal coordinates as

$$\mathbf{s} = D(\Delta\Lambda^2 + e\Delta\Theta^2)$$

where $\Delta\Lambda^2 = (3/2)(\Lambda^2 - \mathbf{I}\ \mathrm{tr}\ \Lambda^2/3)$ and $\Delta\Theta^2 = (3/2)(\Theta^2 - \mathbf{I}\ \mathrm{tr}\ \Theta^2/3)$, tr and **I** denoting the trace operator and the identity matrix, respectively. The three diagonal components of **s** in terms of principal coordinates are S_x, S_y, and S_z, the first of which is treated only in the present analysis.
(14) Liberman, M. H.; Abe, Y.; Flory, P. J. *Macromolecules* **1972**, *5*, 550.
(15) Flory, P. J. *Rubber Chem. Technol.* **1975**, *48*, 513.
(16) Clement, C. B.; Bothorel, P. *J. Chim. Phys. Phys. Chim. Biol.* **1964**, *61*, 878.
(17) Flory, P. J. *Faraday Discuss. R. Soc. Chem.* **1979**, *68*, 14.
(18) Queslel, J.-P.; Erman, B.; Monnerie, L. *Macromolecules*, following paper in this issue.

Experimental Determination of Segmental Orientation in Polyisoprene Networks by Fluorescence Polarization and Comparison with Theory†

Jean-Pierre Queslel, Burak Erman,‡ and Lucien Monnerie*

Laboratoire de Physicochimie Structurale et Macromoléculaire, Associé au CNRS, ESPCI, 75231 Paris Cedex 05, France. *Received December 27, 1984*

ABSTRACT: Segmental orientation is determined in deformed polyisoprene networks, in equilibrium, containing fluorescent anthracene labels attached to the middle of precursor chains and randomly located between cross-links. Measurements show that orientation depends nonaffinely on macroscopic strain, is not proportional to stress, and decreases rapidly with increasing temperature and dilution. Comparison of results with predictions of the theory based on the real network model shows that observed segmental orientation results from the joint contribution of nonaffine transformations of chains upon deformation and of distortion of the junction constraint domains. Strong temperature and swelling dependence of segmental orientation at all levels of deformation is attributed to local intermolecular correlations of segments.

Introduction

Orientation of segments in an amorphous network results from the deformations of chains under stress. In previous formulations of segmental orientation cited in the preceding paper[1] (referred to as I hereafter), chains have been assumed to deform affinely with the macroscopic strain. Recent experimental work on birefringence[2], and on fluorescence polarization[3,4] of deformed networks has shown that deviations of segmental orientation from the predictions of the affine model are significant. Furthermore, these experiments have shown that local intermolecular orientational correlations of segments with their neighbors contribute to orientation.

Discrepancies between experimental measurements of strain birefringence and the existing affine theories have recently been reviewed.[5] Analysis of the phenomenon of birefringence in terms of the real network model, in which chains transform nonaffinely with macroscopic strain, led to results that were in satisfactory agreement with those of experiment. In the preceding theoretical treatment[1] of segment orientation, similar corrections are applied to the commonly used freely jointed affinely deforming chain model. The resulting expression for the orientation function is seen to be the product of two terms, one showing the effect of individual chain properties, referred to as the configurational factor, the other describing the dependence on macroscopic strain, referred to as the strain function. Additional contributions to orientation, due to local intermolecular correlations, are incorporated into the configurational factor, as suggested by birefringence and fluorescence polarization experiments.

With improved techniques of experimental spectroscopy,[6,7] the magnitude of the configurational factor and the form of the strain function for amorphous networks may be determined accurately. In this study we report results of fluorescence spectroscopy on polyisoprene networks under uniaxial tension and compare them with predictions of the theory. The networks used contain a small number of chains labeled with a fluorescent group (anthracene), the orientation of which is determined by the measurement of fluorescence polarization induced upon deformation.

Materials and Methods

Samples were generously provided by Manufacture Michelin. Unimodal networks (samples A and B) were formed from an anionic commercial polyisoprene Shell IR 307 with a high cis-1,4 configuration (92% cis, 5% trans) (T_g(DSC) = −60 °C) of high molecular weight ($M_n = 46.3 \times 10^4$, $M_w = 182 \times 10^4$).

Bimodal networks (samples C and D) were formed from blends of 75% w/w IR 307 and 25% polyisoprene chains of low molecular weight (M_n = 50 000), the microstructure of which is similar to that of IR 307.

Labeled anionic polyisoprene chains were prepared by using a method analogous to that reported previously for polystyrene.[8] Monofunctional "living" chains of molecular weight 300 000 were synthesized and deactivated by 9,10-bis(bromomethyl)anthracene. Each of the resulting chains of double molecular weight contains a dimethylanthracene (DMA) fluorescent group at its center. Thus the fluorescent transition moment, the orientation of which is measured, lies along the chain axis.

The labeled polymer (1%) and the matrix (99%), carefully purified by extraction with ethanol, were mixed in solution. Samples were molded and cross-linked with dicumyl peroxide. Curing time and temperature were adjusted to get different cross-linking densities, which were characterized by the average molecular weight M_c of network chains (between adjacent junctions) derived from measurements of the equilibrium swelling ratio in cyclohexane and through the classical Flory–Rehner equation.

† This paper is dedicated to Dr. Pierre Thirion on the occasion of his retirement.
‡ Permanent address: Bogazici University, Bebek, Istanbul, Turkey.

0024-9297/85/2218-1991$01.50/0